Validation of the Transporter Ligand Cyanoimipramine as a Marker of Serotonin Innervation Density in Brain

Jean-Paul Soucy, Francine Lafaille, Pierrette Lemoine, Abdelghani Mrini and Laurent Descarries

Département de Médecine Nucléaire, Hôpital Notre-Dame and Département de Pathologie et Centre de Recherche en Sciences Neurologiques, Université de Montréal, Montréal, Canada

Radiolabeled ligands of monoamine transporters have already been used to visualize cerebral monoamine innervation by tissue autoradiography and by PET or SPECT in vivo. **Methods:** A sampling technique was developed to allow for both the autoradiographic counting of serotonin (5-HT) axonal varicosities, labeled by uptake and storage of [^{3}H]5-HT, and the measurement of the binding of [^{3}H]cyanoimipramine ([^{3}H]CYI), a specific 5-HT transporter ligand, in adjacent slices of adult rat neostriatum. The experiments were conducted in normal, decreased (after 5,7-dihydroxytryptamine lesions in adults) or increased (after 6-hydroxydopamine lesions in neonates) states of neostriatal 5-HT innervation. **Results:** In normal tissue, the regional density of [^{3}H]CYI binding faithfully reproduced rostrocaudal variations in the number of [^{3}H]5-HT-labeled axonal varicosities. Pairs of values from all three experimental groups showed a highly significant linear correlation ($r = 0.93$) between the density of [^{3}H]CYI binding and the number of 5-HT varicosities per cubic millimeter of tissue. The intercept of the regression line was close to zero; this confirmed the selectivity of the ligand. **Conclusion:** Under drug-free conditions, specific [^{3}H]CYI binding is a good quantitative index of 5-HT innervation density in brain tissue and is not significantly up- or downregulated on 5-HT denervation or hyperinnervation. When it is adequately labeled, such a ligand might therefore be appropriate to quantify regional 5-HT innervation in vivo by PET or SPECT. The present approach should also be useful to select ligands to quantify 5-HT and monoamine systems.

Key Words: monoamines; terminals; monoamine innervation, quantification of; PET; SPECT

J Nucl Med 1994; 35:1822–1830

Reuptake into axon varicosities (or terminals) by transporters present on the nerve cell membrane is a major mode of inactivation for biogenic amine transmitters [dopamine, norepinephrine and serotonin (5-HT)] released in the central or the peripheral nervous system (*1,2*). Drugs that specifically recognize and block these transporters have therefore been developed to increase transmitter availability in the pathologic conditions that are assumed to result from a decreased efficacy of monoamine transmission. Among others, 5-HT reuptake blockers, such as fluoxetine, sertraline, fluvoxamine and paroxetine, have become widely used in the treatment of severe depression (*3–6*).

Monoamine transporter blockers have another clinical application as radiotracers that allow visualization of transmitter reuptake sites by PET (*7–12*) or SPECT (*12–16*). Many such compounds have already been successfully imaged in laboratory animal and human brain, which demonstrated their potential usefulness for pathophysiologic studies, diagnosis and management of neurodegenerative and psychiatric diseases and the investigation of substance abuse. Thus far, these radiopharmaceuticals provide the only practical means to evaluate the density of a monoamine innervation in vivo, even though other alternatives may be envisaged (*17*).

A basic tenet of such imaging studies is that the amount of binding to the transporter in different regions of the brain is proportional to the respective density of innervation by the corresponding monoamine system. Several membrane binding and/or autoradiographic investigations of brain tissue have indeed shown that, under conditions of severe 5-HT or dopamine denervation, for example, the respective recognition sites are decreased in number or no longer visualized (*7,18–30*). They will reappear after intracerebral grafting and reinnervation by the same type of fetal neurons (*31–34*). In vivo studies with PET (*35,36*) have yielded similar results in various experimental models and parkinsonian brain. However, it has not yet been proved that the loss of monoamine reuptake sites (at axon varicosities or terminals) is actually accompanied by a proportional decrease in ligand binding. Moreover, the semiquantitative approach of these studies does not rule out possible up- or downregulation of the transporter recognition sites in conditions of decreased or increased innervation density, as commonly observed with transmitter receptor sites.

In this context, the quantitative relationship between the local binding of a highly specific 5-HT transporter ligand, cyanoimipramine (CYI), and the density of the correspond-

Received Dec. 8, 1993; revision accepted June 23, 1994.

For correspondence or reprints contact: L. Descarries, MD, Département de Pathologie, Université de Montréal, CP 6128, Succursale A, Montréal, Quebec, Canada H3C 3J7.

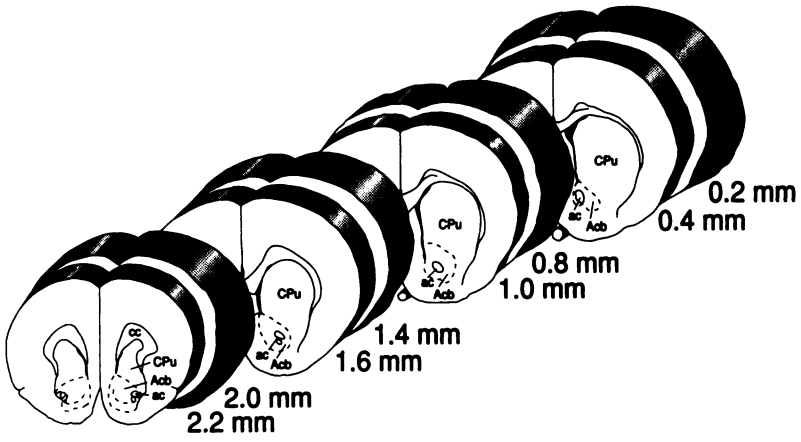

FIGURE 1. Schematic representation of sampling procedure used to process adjacent vibratome slices of neostriatum for [^{3}H]5-HT uptake/storage and [^{3}H]CYI binding autoradiography. Transverse slices, 200 and 400 μm in thickness, respectively, were taken at indicated distances rostral to bregma (in millimeters). ac = anterior commissure; Acb = accumbens nucleus; cc = corpus callosum; CPu = caudate-putamen or neostriatum.

ing innervation (5-HT) was evaluated by two independent autoradiographic approaches. A sampling procedure was developed to examine the same region of rat brain for both the number of 5-HT axonal varicosities (labeled by uptake and storage of [^{3}H]5-HT) and for the amount of specific [^{3}H]CYI binding. The neostriatum was a region of choice for these experiments because it is relatively large and normally shows a well-documented rostrocaudal increasing gradient in 5-HT innervation density. Furthermore, its 5-HT innervation density can be experimentally varied from almost 0% to 200% of its normal density. Lastly, as a territory of 5-HT projection remote from its nerve cell bodies of origin, it is representative of forebrain regions innervated by monoamine neurons.

MATERIALS AND METHODS

Experimental Groups

Sprague-Dawley rats of both sexes were divided into three groups as follows: (1) normal controls, (2) 5-HT-denervated after 5,7-dihydroxytryptamine (5,7-DHT) lesions as adults and (3) 5-HT-hyperinnervated after neonatal lesions with 6-hydroxydopamine (6-OHDA).

The normal controls (n = 9) were purchased a few days prior to experiments and weighed 200 to 600 g at the time of sacrifice.

The 5-HT-denervated rats (hypoinnervated neostriatum, n = 10) were subjected to unilateral lateroventricular administration of 5,7-DHT as young adults. After a double pretreatment with nomifensine [15 mg/kg intraperitoneally (i.p.) 45 min earlier] and desmethylimipramine (15 mg/kg i.p., 45 min earlier) to protect dopamine and norepinephrine neurons, respectively, they were anesthetized with a 5:1 mixture of ketamine and xylazine and injected into the right lateral ventricle, over a period of 5 min, with 400 μg (p.w.) of 5,7-DHT creatinine sulfate dissolved in 20 μl of saline containing 0.1% ascorbic acid. The stereotaxic coordinates were A = −8.0 mm bregma, L = 1.5 mm and H = 4.0 mm below dura mater (*37*). These rats were studied 3 to 6 weeks later, at a time when they weighed 300 to 525 g.

The rats with excessive 5-HT innervation of the neostriatum (hyperinnervated, n = 5) were treated according to the technique initially reported by Stachowiak et al. (*38*) but under stereotaxic control (*39*). In brief, female rats were purchased pregnant and individually housed with free access to food and water. Three days after delivery, the pups were anesthetized with ether and by cooling on ice and given bilateral cerebroventricular injections of 6-OHDA hydrochlorate, 50 μg f.b. in 5 μl of 0.9% NaCl that contained 0.1% ascorbic acid on each side after pretreatment with desmethylimipramine (25 mg/kg, 45 min earlier subcutaneously). The stereotaxic coordinates were A = 0 mm bregma, L = 1.5 mm and H = 3.3 mm below the skull surface. The pups were returned to their mothers and housed in groups under standard conditions to be studied as adults, 3 and 6 mo later, at a time when they weighed 180–290 g.

Alternate Tissue Sampling for Monoamine Uptake and Storage and for Ligand Binding Autoradiography

After deep anesthesia with pentobarbital (65 mg/kg i.p.), every rat was perfused with ice-cold artificial cerebrospinal fluid (CSF) (*40*). The whole brain was rapidly removed and placed in a cutting holder and 3- to 4-mm thick transverse blocks that encompassed the entire neostriatum were excised from each hemisphere. The blocks were immediately cut with a vibratome filled with melting CSF ice. After trimming, four pairs of alternate 200- and 400-μm transverse slices were obtained, starting from an anatomic level equivalent to stereotaxic plane A = 2.2 ± 0.5 mm bregma rostrally and ending at about A = −0.2 mm ± 0.5 mm bregma caudally (Fig. 1). The 200-μm thick slices were transferred to numbered vials containing ice-cold CSF, and the matching 400-μm thick slices were laid flat on glass slides covered with embedding medium, frozen on dry ice and kept at −80°C until subsequent sectioning.

Tritium-3-5-HT Uptake and Storage Labeling, Semithin-Section Autoradiography and Counting of Serotonin Axon Terminals

The procedure was essentially as described in detail by Doucet and Descarries (*41*). The [^{3}H]5-HT labeling was carried out in an oscillating water bath warmed to 37°C, under a 95% O_2/5% CO_2 atmosphere. The 200-μm thick slices were first preincubated for 15 min in artificial CSF supplemented with dextrose 1%, oxygenated with the 95% O_2/5% CO_2 mixture, which contained 0.1 m*M* pargyline (Sigma, a monoamine oxidase inhibitor) and 10 μ*M*

benztropine (Sigma, a blocker of uptake by dopamine neurons). Tritium-3-5-HT (DuPont; [1,2-^{3}H(N)]5-hydroxytryptamine creatinine sulfate, 925–1014 GBq/mmole) was then added at a final concentration of 1.0 μM for an incubation of 15 min, which was stopped by rapid cooling to near 0°C. The slices were then fixed for 20 min at the bottom of vials that contained 3.5% glutaraldehyde in 0.1 M phosphate buffer, mounted on glass slides, post-fixed with osmium tetroxide vapors for 2 hr, detached from the slides during dehydration in a graded series of ethanol, infiltrated with propylene oxide-epoxy resin mixtures and flat-embedded in epoxy resin at the bottom of cubic plastic molds.

After polymerization, each 200-μm thick slice was autoradiographed as a small series (*2–4*) of 4-μm thick sections, which were cut with a microtome for large, hard objects. These semithin sections were mounted on silanized glass slides, coated by dipping in liquified emulsion (Ilford K-5 diluted 1:1 in distilled water), exposed for 29 days and developed in D-19. The labeled varicosities (aggregates of silver grains) were counted directly from these autoradiographs, using a Leitz-Wetzlar photomicroscope equipped with a ×16 PlanApo lens and connected through a video camera (Panasonic WV-BD400; 768 × 493 pixels for 1.7 cm^2) to a computerized image analysis system. In any given slide, counts were obtained from three to six small rectangular fields measuring 350 × 490 μm (0.17 mm^2), within each of three predetermined neostriatal sectors in which the density of [^{3}H]CYI binding would also be measured in film autoradiographs of adjacent sections (Fig. 2).

After dipgitization of these microscopic fields, the gray scale was adjusted to segment the images into grain aggregates versus other features (Fig. 3A and B). Correction for feature fusion was carried out as described by Doucet et al. (*40*), who had determined by light microscopy the average number of [^{3}H]5-HT varicosities represented by binary image features of various sizes.

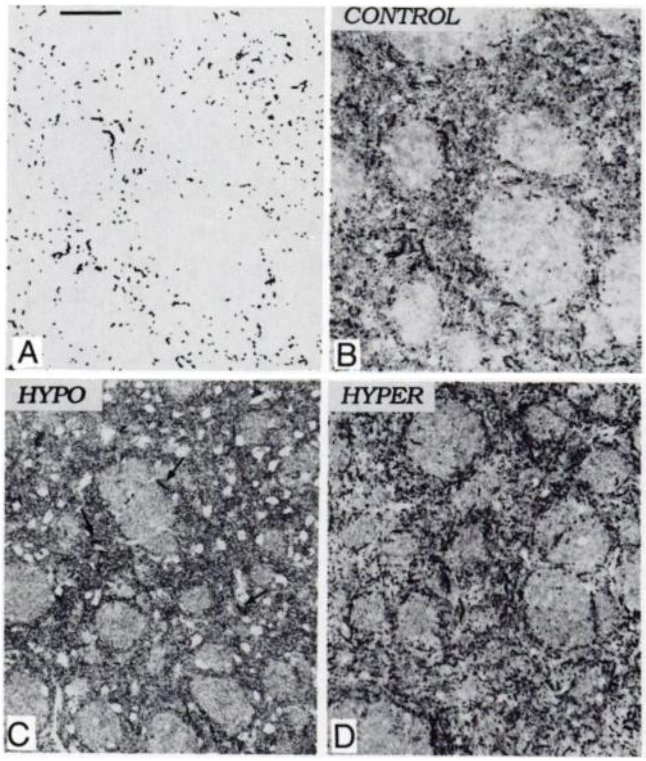

FIGURE 3. Micrographs photo illustrating material used for counting [^{3}H]5-HT-labeled axonal varicosities after 29 days of autoradiographic exposure. (A–D) See Materials and Methods for technical details. A is the digitized image of B (normal neostriatum) as printed at the time of the counts. (C) After 5,7-DHT denervation, most of typical small and dense aggregates of silver grains have disappeared. Very few clusters are still present (arrows) over diffuse scattering of isolated grains in background. In contrast, in 5-HT-hyperinnervated neostriatum after neonatal 6-OHDA (D), there is a marked increase in the number of clusters compared with the comparable area of control (B) (×160). Scale bar = 100 μm.

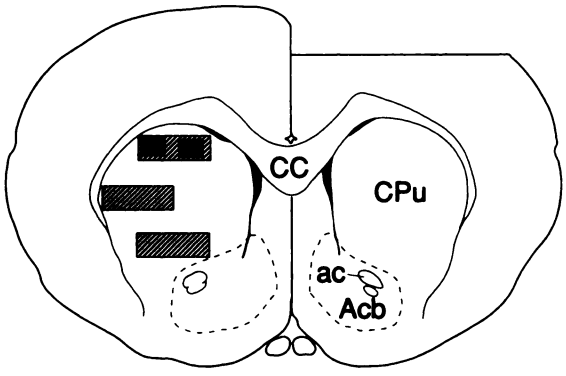

FIGURE 2. Approximate location of predetermined neostriatal sectors subjected to both densitometric measurement of specific [^{3}H]CYI binding and granulometric counting of [^{3}H]5-HT-labeled axonal varicosities, as described in Materials and Methods. Three large rectangles outline 0.87-mm^2 areas from which single densitometric readings were obtained; smaller fields drawn within the upper rectangle exemplify the smaller fields (0.17 mm^2) in which varicosities were counted.

The initial results were recorded as numbers of labeled sites per surface unit (in square millimeters) of autoradiograph. Two correction factors were then applied to convert these counts into number of varicosities per cubic millimeter of tissue. First, to compensate for incomplete autoradiographic detection at the chosen exposure time, the counts were transformed with the ratio between the number of silver grain aggregates at this particular exposure time (29 days) and the theoretic maximum extrapolated from a calibration curve (Fig. 4). Second, to compensate for the incomplete detection of tritium beta particles from 4-μm thick sections, the resulting values were further transformed into their equivalent for a tissue thickness of 0.5 μm, fully transparent to tritium emission (*40*). Extrapolation to a volumetric unit of tissue (cubic millimeters) was then obtained from the stereologic formula $N = n'' \times 1000/(t + d - 2h)$, where n'' is the doubly transformed value per square millimeter of autoradiograph; t is the 0.5-μm tissue thickness; d the mean diameter of labeled neostriatal 5-HT varicosities as measured by electron microscopy (*42*); and h the height of lost caps, i.e., the top portions of labeled varicosities insufficiently large to induce a detectable signal (*43*).

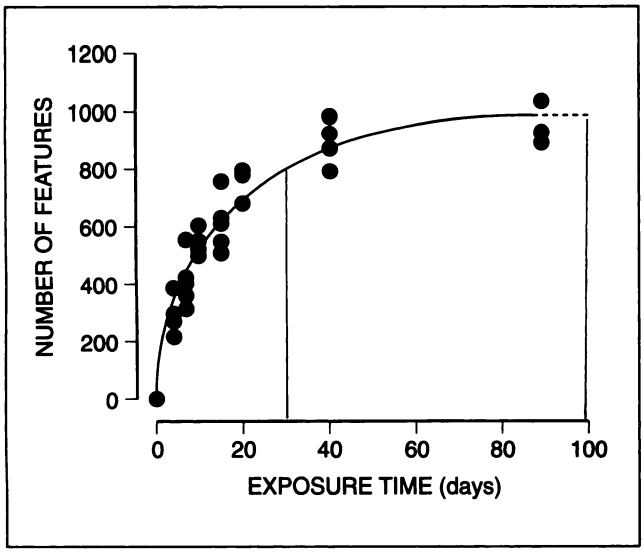

FIGURE 4. Number of [^{3}H]5-HT-labeled axonal varicosities visualized in autoradiographs of neostriatum as function of autoradiographic exposure time. Counts from given neostriatal sector were obtained from adjacent sections at different time points, and three to five series were obtained from different slices. Seventy-two percent of the theoretical maximum (infinite exposure) was attained after 29 days.

Tritium-3-CYI Binding, Film Autoradiography and Densitometric Measurements

To emulate conditions expected from in vivo human studies, [^{3}H]CYI binding was carried out at 37°C. Neostriatal membranes were prepared as follows. Rats that weighed 225 to 275 g were killed by decapitation, and the neostriatum was promptly dissected over ice. The tissue was homogenized in 20 volumes of cold CSF for 17 sec at 8000 rpm (Brinkman Polytron PT 3000, Kinematica AG) and centrifuged at 34,000 g for 10 min at 4°C. The pellets were reprocessed twice in the same fashion and frozen at −80°C until used.

Tritium-3-CYI binding was performed in 0.5-ml aliquots of artificial CSF that contained membranes from 1.15 mg of fresh tissue. The tritiated ligand (ARC; 3-[N-methyl-^{3}H]cyanoimipramine hydrochloride, 3.1 × 10^3 GBq/mmole) was used at a final concentration of 0.5 n*M*. The nonspecific binding was defined by adding 10 μM fluoxetine hydrochloride to the incubating medium. Incubation was ended by filtration followed by three 4-ml rinses of CSF over glass fiber discs under a high vacuum. In these conditions, maximum specific binding was attained after an incubation time of 10 min and remained stable for at least 1 hr (Fig. 5).

The 400-μm thick frozen slices from intact, denervated or hyperinnervated neostriatum were cut into 20-μm thick cryostat sections, which were mounted on chromalum-gelatin-coated slides and stored at −80°C until used. After they were thawed, these sections were preincubated at 25°C for 15 min and incubated at 37°C for 20 min in CSF solution that contained 0.5 n*M* [^{3}H]CYI with or without 10 μM fluoxetine hydrochloride to evaluate nonspecific binding later. The slides were then washed (4 × 5 min) in CSF at 4°C, quickly rinsed in water, dried under a stream of cold air and apposed to tritium-sensitive film ([^{3}H] Hyperfilm, Amersham), together with [^{3}H] microscales (Amersham). The autoradiographic exposure lasted for 26 days, and the films were developed with D-19.

These autoradiographs were examined with a dedicated computerized image analysis system (MCID, Imaging Research). From each slide studied, single densitometric measurements were obtained in three predefined sectors of the neostriatum, mediodorsal, laterointermediate and medioventral, as illustrated in Figure 2. Each of these fields measured 1.52 × 0.57 mm (0.87 mm^2). Nonspecific binding was measured in adjacent sections, and specific binding was obtained by substraction of the nonspecific binding from the total binding. Standardization curves generated from the microscales were used to convert optical density readings to femtomoles per milligram of protein. Anatomic landmarks were recorded on schematic drawings to allow identical repositioning of the nearby 4-μm thick sections examined by [^{3}H]5-HT uptake/storage autoradiography.

Data Correlation

The alternate sampling protocol made it possible to estimate the density of 5-HT innervation and the amount of specific [^{3}H]CYI binding in matching neostriatal sectors distant by 600 μm at most rostrocaudally. Analysis of the data was performed with a commercially available statistics package (StatView, Abacus Concepts). A simple linear correlation was sought, and the statistical significance was set at the $p < 0.05$ level. After technically unsuitable material was rejected, it was possible to match 53 data pairs from control, 43 from hypoinnervated and 20 from hyperinnervated neostriatum, a total of 116 data pairs. Unpaired t-tests were used to compare means within or between groups.

RESULTS

Counts of [^{3}H]5-HT-Labeled Terminals

Figure 3 illustrates the autoradiographic appearance of the 5-HT innervation labeled by uptake and storage of [^{3}H]5-HT in control, 5-HT-hypoinnervated and 5-HT-hyperinnervated neostriatum. At such a working magnification, individual axonal varicosities were readily visualized as small and dense aggregates of silver grains (clusters) over a background of dispersed grains. Many clusters were closely aligned in short linear or curved segments, which represented several varicosities along the same axonal segment. As previously described (*42*), most of these clusters

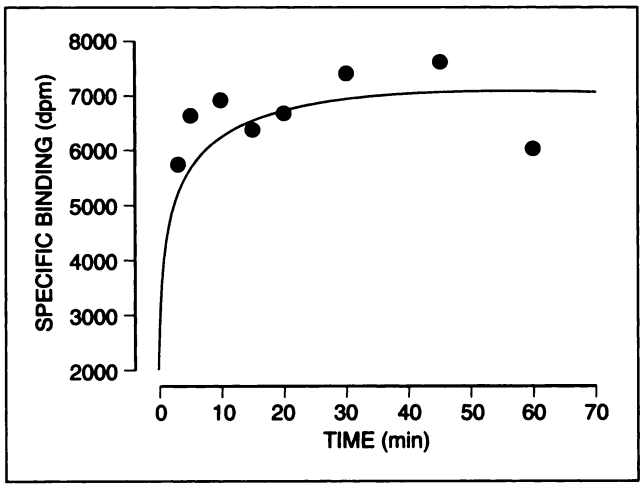

FIGURE 5. Kinetics of [^{3}H]CYI binding to rat neostriatal membranes under conditions of present experiments (see Materials and Methods for technical details).

were found in the neuropil, in between the myelinated fascicles of the internal capsule.

Differences were visually apparent between control, 5-HT-hypoinnervated and 5-HT-hyperinnervated tissue. After 5,7-DHT denervation, only a few clusters were still visible over the diffuse background of dispersed grains (Fig. 3B). After neonatal 6-OHDA lesion and 5-HT hyperinnervation (Fig. 3C), the number of clusters was much greater than in a comparable anatomic sector of control neostriatum (Fig. 3A).

As measured with [^{3}H]5-HT uptake autoradiography, the 5-HT innervation density in control neostriatum ranged from 0.8 to 7.7 × 10^6 varicosities per cubic millimeter of tissue, averaging 5.4 ± 1.5 × 10^6. As previously reported (*42*), most rostral values (n = 8) were significantly lower than the most caudal ones (n = 10; 4.5 ± 0.4 × 10^6 versus 5.9 ± 0.9 × 10^6, respectively; $p < 0.001$). In hypoinnervated tissue, the values ranged from 0.1 to 6.8 × 10^6/mm^3 varicosities, for an average of 1.0 ± 1.7 × 10^6, which represented an 81% decrease from control ($p < 0.001$). In hyperinnervated tissue, the number of varicosities ranged from 4.6 to 10.7 × 10^6, with an average of 8.0 ± 1.8 × 10^6. Again, that value was markedly different from control (48% increase, $p < 0.001$).

As can be seen from Figure 6, there was some overlap between the three animal groups. Seven of 53 values from the controls were more than 1 s.d. below the mean of that group (3 were 2 s.d. below) and 6 were more than 1 s.d. above. In the hypoinnervated group, there were 4 of 43 values within 1 s.d. and 5 within 2 s.d. from the mean of controls. Eleven of the 20 hyperinnervated values were within 2 s.d. from that mean, including 5 within 1 s.d.

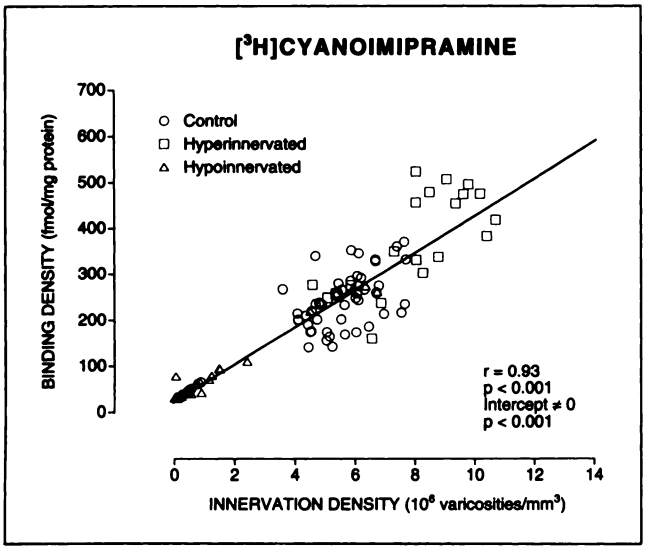

FIGURE 6. Graphic representation of regression analysis of [^{3}H]CYI specific binding versus number of [^{3}H]5-HT-labeled axonal varicosities in corresponding sectors of neostriatum. The 116 data pairs are from tissue showing normal, reduced or excessive density of 5-HT innervation. Data are closely fitted by a linear function intersecting the origin near zero.

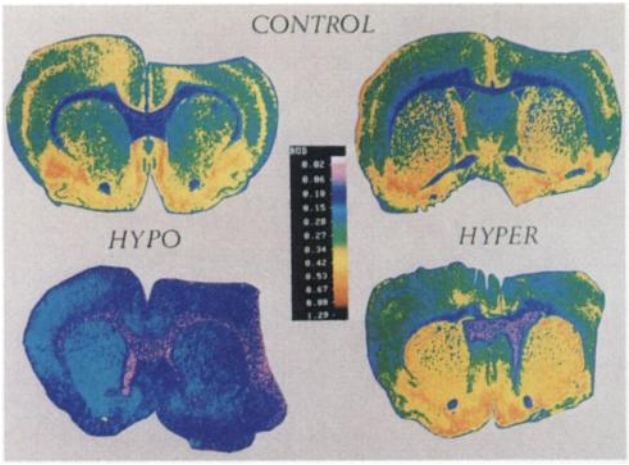

FIGURE 7. Color-coded images of film autoradiographs used for measurement of specific [^{3}H]CYI binding. Pictures were taken directly from the screen of the image analysis system. Note increased density of binding in caudal compared with rostral half of normal neostriatum (right versus left control); reduced (almost null) density of binding throughout forebrain of a 5,7-DHT-lesioned rat (hypoinnervated); and considerable increase by comparison to control in rostral neostriatum of a rat neonatally lesioned with 6-OHDA (hyperinnervated).

Densitometric Measurements of Specific [^{3}H]CYI Binding

Figure 7 illustrates the typical appearance of specific [^{3}H]CYI binding in control, hypoinnervated and hyperinnervated tissue, as photographed directly from the screen of the image analysis system after subtraction of nonspecific values and color coding. Nonspecific binding was low; it represented less than 15% of the total binding in control tissue. Considerable differences in regional binding densities were visually apparent in control and hyperinnervated tissue. In transverse sections of control neostriatum, increasing dorsoventral, mediolateral and rostrocaudal gradients could be observed (Fig. 7, top panels), as already described for 5-HT innervation density (*42*). Marked laminar differences were also visible in the cerebral cortex, as previously reported (*44*).

The differences between control, hypo- and hyperinnervated neostriatum were again striking (Fig. 7). In eight rats treated with intraventricular 5,7-DHT, [^{3}H]CYI binding was a little above the background level throughout the neostriatum and in the rest of forebrain. There were two rats in which denervation was less complete, at least in some sectors of neostriatum. In the five rats neonatally treated with 6-OHDA, most sections showed obvious increases in [^{3}H]CYI binding density that were particularly obvious in the rostral neostriatum.

In control neostriatum, specific [^{3}H]CYI binding ranged from 61 to 371 fmole/mg of protein and averaged 233 ± 72 fmole. Most rostral readings displayed an average binding density of 212 ± 41 fmole/mg of protein compared with 281 ± 43 fmole for the most caudal (n = 10, p = 0.003); this 33% difference closely matched the 31% increase in innervation density described earlier. In hypoinnervated tissue,

the values ranged from 29 to 273 fmole/mg of protein, for an average of 67 ± 64 fmole, which represented a 71% decrease from control ($p < 0.001$). This difference was also comparable to the decrease in innervation density described previously (81%). In hyperinnervated tissue, the range of binding densities was 159 to 524 fmole/mg of protein, for an average of 372 ± 109 fmole. This 60% difference from control values was again highly significant ($p < 0.001$) and somewhat higher than the measured increase in innervation density (48%).

As observed for innervation density, Figure 6 revealed overlap of [^{3}H]CYI binding values between the three groups. Six of 53 values from the controls were more than 1 s.d. below the mean of that group (3 were 2 s.d. below), and 8 were more than 1 s.d. above. In the hypoinnervated group, there were 4 of 43 values within 1 s.d. and 7 within 2 s.d. of the mean of controls. Ten of the 20 hyperinnervated values were within 2 s.d. from that mean, including 7 within 1 s.d.

Correlation Analysis

As shown in Figure 6, the linear-regression analysis of the 116 pairs of data relating [^{3}H]CYI binding density to 5-HT innervation density in control (53 pairs from 9 rats), hypoinnervated (43 pairs from 10 rats) and hyperinnervated neostriatum (20 pairs from 5 rats) indicated a high level of correlation. The coefficient of correlation was 0.93 ($p < 0.001$) and the intercept on the ordinate was close to zero (26 fmole/mg of protein, 95% confidence interval 0.11–41 fmole/mg of protein).

Figure 6 indicates that some of the attempts to modify the density of 5-HT innervation had not been successful in a few animals of both the hypo- and hyperinnervated groups. These data points were kept, however, because they were as useful as others for the particular purpose of the present experiments.

DISCUSSION

These results provide the first demonstration of a close relationship between the amount of specific ligand binding to a monoamine transporter and the actual number of axonal varicosities of the corresponding type in a given region of brain, as established by truly quantitative, independent approaches.

Methodologic Considerations

Earlier studies have given detailed accounts of the autoradiographic method used here for the direct counting of 5-HT axonal varicosities (*40–42*). This method has already been used extensively in adult rat cerebral cortex, hippocampus and neostriatum to obtain quantitative data on the dopamine, norepinephrine and 5-HT innervations (*40,42,45–47*). The values here reported for the density of neostriatal 5-HT innervation in normal adult rat were significantly higher than previously found in the authors' laboratory using the same approach (5.4×10^6 versus 2.6×10^6/mm^3 terminals) (*42*). This difference seemed partly attributable to improvements in the tissue preparative technique but also to the availability of an image analyzer with a finer resolution. In spite of the higher average values reported here, a comparable increasing rostrocaudal gradient was measured in both studies (31% and 29% increases), which was also consistent with a scaling effect of presumed technical origin.

The conditions that allowed specific [^{3}H]CYI binding to 5-HT transporter sites were slightly modified from those of Kovachich et al. (*48*). Incubation with the radioligand was performed at 37°C to approximate in vivo conditions. Based on the previously reported dissociation constant (K_d) for [^{3}H]CYI in adult rat neostriatum, it could be inferred that the occupancy of available sites was about 80% in the present experiments. Consequently, the mean binding density measured in control neostriatum (233 ± 72 fmole/mg of protein) was in excellent agreement with the previous B_{max} value of 345 ± 50 fmole/mg of protein, also derived from autoradiographic measurements in tissue slices. The current average value of 67 fmole/mg of protein for 5-HT-hypoinnervated neostriatum was also consistent with the previously reported B_{max} of 80 fmole/mg of protein for 5,7-DHT-denervated brain tissue other than nucleus raphe dorsalis (*48*).

Correlation of [^{3}H]CYI Binding with 5-HT Innervation Density

Earlier evaluations of transporter ligand and 5-HT innervation properties provided suggestive evidence of a close relationship between 5-HT innervation density and the amount of specific binding for different blockers of 5-HT reuptake in brain tissue. Losses of tritiated indalpine, paroxetine, citalopram or 6-nitroquipazine binding have been documented after more or less severe cytotoxic 5-HT lesions (*19–22*). After 5-HT denervations evidenced by profound depletions of 5-HT content, proportional reductions in the binding of [^{11}C]McN-5652Z and of [^{3}H]paroxetine have been measured (*7,23*). Much less information was available in regard to 5-HT hyperinnervation. In a concurrent biochemical study of 5-HT metabolism carried out in the dopamine-denervated and 5-HT-hyperinnervated neostriatum of neonatally 6-OHDA-lesioned rats, a significant increase in neostriatal [^{3}H]citalopram binding was shown after 3 mo of survival, but it was not found to be proportional to the increase in 5-HT content (*49*). This study also revealed that, 1 mo after the lesion, at a time when the neostriatum is not yet 5-HT hyperinnervated (unpublished observations), the 5-HT content is already elevated but not the [^{3}H]citalopram binding. This is a reminder that indirect indices of 5-HT innervation density have to be interpreted with caution.

Two major aspects of the relationship between [^{3}H]CYI binding and number of [^{3}H]5-HT-labeled axonal varicosities were of crucial importance to establish that [^{3}H]CYI binding could serve as a truly quantitative index of 5-HT innervation density. The first was the actual fidelity or closeness with which this binding reflected known differences in innervation density within or between brain re-

gions. In this regard, it was reassuring to measure a 33% difference in the amount of [^{3}H]CYI binding between the caudal versus rostral neostriatum of normal rat, which was almost identical to the 31% difference in density of 5-HT innervation. It was essential to also investigate whether such a relationship would remain stable under conditions of decreased or increased density of 5-HT innervation or whether some regulatory mechanism would then compensate for or adapt to these changes, as was repeatedly shown to be the case for monoamine transmitter receptors (*50–55*).

Moreover, in the case of 5-HT, not only has upregulation of receptors been reported after denervation or chronic treatment with selective antagonists but also several 5-HT receptor subtypes presumably not carried by the 5-HT terminals themselves have actually been found to be increased in brain regions that show a 5-HT hyperinnervation (*56–58*). Admittedly, reduced 5-HT innervation might be more representative of clinical situations than hyperinnervation, but this latter phenomenon should not be dismissed a priori as the possible accompaniment of certain pathologic or therapeutic states. Moreover, the study of the 5-HT-hyperinnervated tissue provided a wider range of values to define the regression equation that linked [^{3}H]CYI binding with the 5-HT innervation density.

The high correlation coefficient obtained for the full range of values from almost null to more than twice the normal density of neostriatal 5-HT innervation clearly demonstrated that there were no significant changes in the amount of [^{3}H]CYI binding per 5-HT varicosity under these conditions. This does not preclude the possibility that pharmacologic conditions, such as chronic treatment with a 5-HT uptake blocker or monoamine oxidase inhibitor, induce regulation of the expression of the 5-HT transporter as a whole or differentially affect the part(s) of its structure that serve(s) as recognition site. Functional regulation of the 5-HT transporter could then take the form of affinity changes toward certain ligands and not others under a variety of pharmacologic conditions, which remain to be defined more thoroughly (*59–62*). The expression or affinity of other molecules distinct from the 5-HT transporter itself but that interact with it might also be influenced by pharmacologic treatments. For example, the high-affinity binding site for imipramine (and hence probably that of other tricyclic antidepressants), which is distinct from the 5-HT recognition site of the 5-HT transporter, has been shown to be downregulated on chronic treatment with imipramine itself or with monoamine oxidase inhibitor (*63–67*), without a concomitant decrease in 5-HT transport efficacy (*67*). Moreover, the high-affinity binding site for imipramine could have its own endogenous ligand (*67*), which might in turn control 5-HT reuptake independently from variations in the number of 5-HT transporter sites. Other drugs that might act at least partially through such a mechanism are desmethylimipramine and sertraline (*68*).

However, the results of many other studies would seem to argue against possible regulation of the 5-HT transporter under a variety of circumstances. Uptake of [^{3}H]5-HT by brain synaptosomes in animals chronically treated with citalopram (another powerful 5-HT uptake inhibitor) (*69*); binding of [^{3}H]paroxetine to rat cerebral cortical membranes in animals that received tricyclic antidepressants (*70*), citalopram or monoamine oxidase inhibitor (*71*); and binding of [^{3}H]CYI to rat brain slices after in vivo treatment with 5-HT uptake blockers (citalopram and sertraline) or monoamine oxidase inhibitor (*72*) have all been found to remain stable compared with control. Using a different approach, Dewar et al. (*73*) were able to demonstrate that the binding of [^{3}H]paroxetine was regionally decreased in rat brain when a fall in the local concentration of 5-HT was induced by p-chloroamphetamine lesioning of 5-HT terminals but not after comparable 5-HT depletions induced by p-chlorophenylalanine, an inhibitor of 5-HT synthesis that leaves the 5-HT neurons structurally intact.

The second major inference from the present results was that a complete disappearance of the neostriatal 5-HT varicosities results in an almost complete absence of [^{3}H]CYI binding. Although not zero in a strict sense, the intercept of the regression line that linked the two parameters was close to zero. While this result provides a striking demonstration of the selectivity of the [^{3}H]CYI ligand, it also indicated that eventual 5-HT transporter sites located on glia (*74*) would not interfere with the [^{3}H]CYI binding measurements. Unless they were sufficiently distinct from the neuronal transporter not to be recognized by CYI, either such sites represented a small proportion of the total number of 5-HT transporters in neostriatum or they were down- and upregulated proportionally to the density of 5-HT innervation. In any event, the close correlation between [^{3}H]CYI binding and 5-HT innervation density, even at low values, is noteworthy because some monoamine degenerations (e.g., dopamine) become clinically manifest only after severe degrees of denervation are attained (*75*).

CONCLUSIONS

Thus, the amount of specific [^{3}H]CYI binding represents a reliable index of regional 5-HT innervation density in brain tissue, over a wide range of values, at least in drug-free conditions. This could also be true under a variety of pharmacotherapeutic situations that modify 5-HT metabolism or reuptake, as long as these leave the 5-HT neurons structurally intact.

Other reuptake ligands should eventually be tested for similar purposes, either because of their binding characteristics or of the other properties that make them more attractive for human use in vivo, such as their radiochemical features.

The ultimate goal of such experiments is obviously to achieve measurement of the regional density of 5-HT and other monoamine innervations in the human brain by PET and/or SPECT. As long as the understanding of the regulation of ligand binding to monoamine transporters remains empiric, these procedures will be needed for the prelimi-

nary selection of potential ligands. This will then have to be followed by an in vitro evaluation of their binding characteristics in human tissue (compared with those in rat tissue) and by a modeling of their distribution in living brain. Only then should it become feasible to determine the actual number of monoamine varicosities per unit volume of tissue in the living brain and to apply this knowledge to pathophysiologic study, diagnosis and follow-up of a variety of disease states and their treatment.

ACKNOWLEDGMENTS

The authors thank Sylvia Garcia for technical assistance; Guy Doucet, PhD, for advice on experimental procedures; and Giovanni Battista Filosi, Claude Gauthier and Denis Dicaire for graphic and photographic work. Financial support provided through an R&D program (Lomedic 1.6) at the Faculty of Medicine of the Université de Montréal.

REFERENCES

1. Glowinski J, Axelrod J. Inhibition of uptake of tritiated-noradrenaline in the intact rat brain by imipramine and structurally related compounds. *Nature* 1964;204:1318–1319.
2. Schwartz JH. Synaptic vesicles. In: Kandel ER, Schwartz JH, Jessell TM, eds., *Principles of neural sciences*, 3rd ed. New York: Elsevier; 1991:225–234.
3. Mendels J. Clinical experience with serotonin reuptake inhibiting antidepressants. *J Clin Psychiatry* 1987;48(3 suppl):26–30.
4. Lapierre YD. Controlling acute episodes of depression. *Int Clin Psychopharmacol* 1991;6(suppl. 2):23–35.
5. Boyer WF, Feighner JP. An overview of paroxetine. *J Clin Psychiatry* 1992;53:3–6.
6. Nathan RS, Perel JM, Pollock BG, Kupfer DJ. The role of neuropharmacologic selectivity in antidepressant action: fluvoxamine vs desipramine. *J Clin Psychiatry* 1990;51:367–372.
7. Suehiro M, Scheffel U, Dannals RF, et al. A PET radiotracer for studying serotonin uptake sites: carbon-11-McN-5652Z. *J Nucl Med* 1993;34:120–127.
8. Koeppe RA, Kilbourn MR, Frey KA, et al. Imaging and kinetic modeling of [F-18]GBR 12909, a dopamine uptake inhibitor. *J Nucl Med* 1990;31:720.
9. DaSilva JN, Kilbourn MR, Sherman PS, Pisani TL, Mangner TJ. Synthesis and in vivo evaluation of (±)2-[C-11]methyl-amino-2-methyl-3-phenyl-1-propranolol as a potential radiotracer for PET imaging of serotonin uptake sites [Abstract]. *J Nucl Med* 1992;33:861.
10. Müller L, Foged C, Halldin C, et al. Preparation of [C-11]NNC 722, a potential radioligand for the dopamine uptake system. [Abstract] *J Nucl Med* 1992;33:931.
11. Wong DF, Shaya EK, Yung B, et al. C-11 WIN 35,428 imaging of the dopamine transporter site in living human brain [Abstract]. *J Nucl Med* 1992;33:964.
12. Suehiro M, Ravert HT, Scheffel U, et al. Highly potent indanamine 5-HT uptake blockers as radiotracers for imaging 5-HT uptake sites [Abstract]. *J Nucl Med* 1993;34:234P.
13. Laruelle M, Baldwin RM, Zea-Ponce Y, et al. SPECT imaging of monoamine transporter sites with ^{123}I-CIT [Abstract]. *J Nucl Med* 1992;33:510.
14. Fujita M, Shimada S, Fukuchi K, et al. Selective labeling of the dopamine transporter in vitro and in vivo in the rat brain using [I-125]RTI-55 combined with clomipramine: regional distribution using autoradiography [Abstract]. *J Nucl Med* 1993;34:201P.
15. Goodman MM, Kung MP, Kabalka GW, Kung HF, Meyer MA. Radioiodinated 2β-carboisopropoxy-3β-(4-chlorophenyl)-8-(3E-iodopropen-2-YL)-nortropane: synthesis of a potential radioligand for mapping dopamine reuptake sites by SPECT [Abstract]. *J Nucl Med* 1993;34:235P.
16. Biegon A, Mathis CA, Taylor S, Jagust W. Radioiodinated 5-iodo-6-nitroquipazine as an in vivo ligand for brain serotonin terminals. *Soc Neurosci Abstr* 1992;18:409.
17. Wong FCL, Boja JW, Wong DF, et al. X-ray affinity labelling of dopamine transporter by photoaffinity ligands [Abstract]. *J Nucl Med* 1991;32:1839.
18. Dewar KM, Reader TA, Grondin L, Descarries L. [^{3}H]paroxetine binding and serotonin content of rat and rabbit cortical areas, hippocampus, neostriatum, ventral mesencephalic tegmentum, and midbrain raphe nuclei region. *Synapse* 1991;9:14–26.
19. Bénavidès J, Savaki HE, Malgouris C, et al. Quantitative autoradiography of [^{3}H]indalpine binding sites in the rat brain. I. Pharmacological characterization. *J Neurochem* 1985;45:514–520.
20. De Souza EB, Kuyatt BL. Autoradiographic localization of ^{3}H-paroxetine-labeled serotonin uptake sites in rat brain. *Synapse* 1987;1:488–496.
21. D'Amato RJ, Largent BL, Snowman AM, Snyder SH. Selective labeling of serotonin uptake sites in rat brain by [^{3}H]citalopram contrasted to labeling of multiple sites by [^{3}H]imipramine. *J Pharmacol Exp Ther* 1987;242:364–371.
22. Hashimoto K, Goromaru T. High affinity [^{3}H]6-nitroquipazine binding sites in rat brain. *Eur J Pharmacol* 1990;180:273–281.
23. Scheffel U, Ricaurte GA. Paroxetine as an in vivo indicator of 3,4-methylenedioxymetamphetamine neurotoxicity: a presynaptic serotoninergic positron emission tomography ligand? *Brain Res* 1990;527:89–95.
24. Filloux F, Hunt MA, Wamsley JK. Localization of the dopamine uptake complex using [^{3}H]N-[1-(2-benzo(b)thiophenyl) cyclohexyl]-piperidine ([^{3}H]BTCP) in rat brain. *Neurosci Lett* 1989;100:105–110.
25. Richfield EK. Quantitative autoradiography of the dopamine uptake complex in rat brain using [^{3}H]GBR 12935: binding characteristics. *Brain Res* 1991;540:1–13.
26. Andersen PH. Biochemical and pharmacological characterization of [^{3}H]GBR 12935 binding in vitro to rat striatal membranes: labeling of the dopamine uptake complex. *J Neurochem* 1987;48:1887–1896.
27. Janowsky A, Schweri MM, Berger P, et al. The effects of surgical and chemical lesions on striatal [^{3}H]threo-(±)-methylphenidate binding: correlation with [^{3}H]dopamine uptake. *Eur J Pharmacol* 1985;108:187–191.
28. Dubocovich ML, Zahniser NR. Binding characteristics of the dopamine uptake inhibitor [^{3}H]nomifensine to striatal membranes. *Biochem Pharmacol* 1985;34:1137–1144.
29. Chagraoui A, Bonnet JJ, Protais P, Costentin J. In vivo binding of [^{3}H]GBR 12783, a selective dopamine uptake inhibitor, in mouse striatum. *Neurosci Lett* 1987;78:175–179.
30. Javitch JA, Blaustein RO, Snyder SH. [^{3}H]mazindol binding associated with neuronal dopamine and norepinephrine uptake sites. *Mol Pharmacol* 1984;26:35–44.
31. Blunt SB, Jenner P, Marsden CD. The effect of L-dopa assessed by tyrosine hydroxylase immunochemistry and [^{3}H]mazindol autoradiography. *Neuroscience* 1991;43:95–110.
32. Przedborski S, Levivier M, Kostic V, et al. Sham transplantation protects against 6-hydroxydopamine-induced dopaminergic toxicity in rats: behavioral and morphological evidence. *Brain Res* 1991;550:231–238.
33. Zhu SM, Kujirai K, Dollison A, et al. Implantation of genetically modified mesencephalic fetal cells into the rat brain. *Brain Res Bull* 1992;29:81–93.
34. Savasta M, Mennicken F, Chritin M, et al. Intrastriatal dopamine-rich implants reverse the changes in dopamine D_2 receptor densities caused by 6-hydroxydopamine lesion of the nigrostriatal pathway in rats: an autoradiographic study. *Neuroscience* 1992;46:729–738.
35. Brownell AL, Hantraye P, Elmaleh D, et al. Use of [C-11]2β-carbomethoxy-3β-fluorophenyl tropane ([C-11]CFT) in studying dopamine fiber loss in a primate model of parkinsonism [Abstract]. *J Nucl Med* 1992; 33:946.
36. Tedroff J, Aquilonius SM, Hartvig, et al. Monoamine re-uptake sites in the human brain evaluated in vivo by means of ^{11}C-nomifensine and positron emission tomography: the effects of age and Parkinson's disease. *Acta Neurol Scand* 1988;77:192–201.
37. Paxinos G, Watson C. *The rat brain in stereotaxic coordinates*, 2nd ed., New York: Academic Press; 1986.
38. Stachowiack MK, Bruno JP, Snyder AM, Stricker EM, Zigmond MJ. Apparent sprouting of striatal serotonergic terminals after dopamine depleting brain lesions in neonatal rats. *Brain Res* 1984;291:164–167.
39. Fernandes Xavier FG, Doucet G, Geffard M, Descarries L. Dopamine neoinnervation in the substantia nigra and hyperinnervation in the interpeduncular nucleus of adult rat following neonatal cerebroventricular administration of 6-hydroxydopamine. *Neuroscience* 1993:59:77–87.
40. Doucet G, Descarries L, Audet MA, Garcia S, Berger B. Radioautographic method for quantifying regional monoamine innervations in the rat brain. Application to cerebral cortex. *Brain Res* 1988;441:233–259.
41. Doucet G, Descarries L. Quantification of monoamine innervations by light microscopic autoradiography following tritiated monoamine uptake in brain slices. *Neurosci Prot* 1993;050-09:1–15.
42. Soghomonian JJ, Doucet G, Descarries L. Serotonin innervation in adult rat neostriatum. I. Quantified regional distribution. *Brain Res* 1987;425:85–100.
43. Lapierre Y, Beaudet A, Demianczuk N, Descarries L. Noradrenergic axon

terminals in the cerebral cortex of rat. II. Quantitative data revealed by light and electron microscope radioautography of frontal cortex. *Brain Res* 1973; 63:175–182.
44. Audet MA, Descarries L, Doucet G. Quantified regional and laminar distribution of the serotonin innervation in the anterior half of adult rat cerebral cortex. *J. Chem Neuroanat* 1989;2:29–44.
45. Doucet G, Descarries L, Garcia S. Quantification of the dopamine innervation in adult rat neostriatum. *Neuroscience* 1986;19:427–445.
46. Descarries L, Lemay B, Doucet G, Berger B. Regional and laminar density of the dopamine innervation in adult rat cerebral cortex. *Neuroscience* 1987;21:807–824.
47. Oleskevich S, Descarries L. Quantified distribution of the serotonin innervation in adult rat hippocampus. *Neuroscience* 1990;34:19–33.
48. Kovachich G, Aronson CE, Brunswick DJ, Frazer A. Quantitative autoradiography of serotonin uptake sites in rat brain using [^{3}H]cyanoimipramine. *Brain Res* 1988;454:78–88.
49. Molina-Holgado E, Dewar K, Descarries L, Reader TA. Altered dopamine and serotonin metabolism in the DA-denervated and 5-HT-hyperinnervated neostriatum of adult rat after neonatal 6-hydroxydopamine. *J Pharmacol Exp Ther* 1993: in press.
50. Creese I, Burt DR, Snyder SH. Dopamine receptor binding enhancement accompanies lesion-induced behavioral supersensitivity. *Science* 1977;197: 596–598.
51. Muller P, Seeman P. Brain neurotransmitter receptors after long-term haloperidol: dopamine, acetylcholine, serotonin, α-noradrenergic and naloxone receptors. *Life Sci* 1977;21:1751–1758.
52. Hess EJ, Alners LJ, Le H, Creese I. Effects of chronic SCH23390 treatment on the biochemical and behavioral properties of D_1 and D_2 dopamine receptors: potentiated behavioral responses to a D_2 dopamine agonist after selective D_1 dopamine receptor upregulation. *J Pharmacol Exp Ther* 1986; 238:846–854.
53. Sporn JR, Wolfe BB, Harden TK, Molinoff PB. Supersensitivity in rat cerebral cortex: pre- and postsynaptic effects of 6-hydroxydopamine at noradrenergic synapses. *Mol Pharmacol* 1977;13:1170–1180.
54. U'Prichard DC, Bechtel WD, Rouot BM, Snyder SH. Multiple apparent alpha-noradrenergic binding sites in rat brain: effects of 6-hydroxydopamine. *Mol Pharmacol* 1979;16:47–60.
55. Vos P, Davenport PA, Artymyshyn RP, Frazer A, Wolfe BB. Selective regulation of beta-2 adrenergic receptors by the chronic administration of the lipophilic beta adrenergic receptor agonist clenbuterol: an autoradiographic study. *J Pharmacol Exp Ther* 1987;242:707–712.
56. Roth BL, Hamblin M, Ciaranello RD. Regulation of 5-HT_2 and 5-HT_{1C} serotonin receptor levels. *Neuropsychopharmacology* 1990;3:427–433.
57. Paré M, Descarries L, Quirion R. Up-regulation of 5-hydroxytryptamine$_2$ and neurokinin-1 receptors associated with serotonin/substance P hyperinnervation in the rat inferior olive. *Neuroscience* 1992;51:97–106.
58. Radja F, Descarries L, Dewar KM, Reader TA. Serotonin 5-HT_1 and 5-HT_2 receptors in adult rat brain after neonatal destruction of nigrostriatal dopamine neurons: a quantitative autoradiographic study. *Brain Res* 1993;606: 273–285.
59. Miller KJ, Hoffman BJ. Regulation of the serotonin transporter by PKC and adenosine receptor activation [Abstract]. *Soc Neurosci Abstr* 1993;19:221.
60. Rattray M, Wotherspoon G, Savery D, et al. Fenfluramine and NMDA downregulate serotonin transporter messenger RNA in subdivisions of the rat dorsal raphe complex [Abstract]. *Soc Neurosci Abstr* 1993;19:495.
61. Knight DL, Owens MJ, Morgan WN, Nemeroff CB. Regional differences in ^{3}H-citalopram binding in response to saline injections or fenfluramine-induced lesions [Abstract]. *Soc Neurosci Abstr* 1993;19:498.
62. Little KY, Caroll FI, Duncan GE. Decreased cortical 5-HT binding in depressed humans [Abstract]. *Soc Neurosci Abstr* 1993;19:1884.
63. Raisman R, Briley MS, Langer SZ. Specific tricyclic antidepressant binding sites in rat brain characterised by high-affinity ^{3}H-imipramine binding. *Eur J Pharmacol* 1980;61:373–380.
64. Kinnier WJ, Chuang DM, Costa E. Down regulation of dihydroalprenolol and imipramine binding sites in brain of rats repeatedly treated with imipramine. *Eur J Pharmacol* 1980;67:289–294.
65. Briley M, Raisman R, Arbilla S, Casadamont M, Langer SZ. Concomitant decrease in [^{3}H]imipramine binding in cat brain and platelets after chronic treatment with imipramine. *Eur J Pharmacol* 1982;81:309–314.
66. Zsilla G, Barbaccia ML, Gandolfi O, Knoll J, Costa E. (−)-Deprenyl: a selective MAO "B" inhibitor increases [^{3}H]imipramine binding and decreases β-adrenergic receptor function. *Eur J Pharmacol* 1983;89:111–117.
67. Barbaccia ML, Gandolfi O, Chuang DM, Costa E. Modulation of neuronal serotonin uptake by a putative endogenous ligand of imipramine recognition sites. *Proc Natl Acad Sci USA* 1983;80:5134–5138.
68. Butler J, Tannian M, Leonard BE. The chronic effects of desipramine and sertraline on platelets and synaptosomal 5HT uptake in olfactory bulbectomised rats. *Prog Neuropsychopharmacol Biol Psychiatry* 1988;12:585–594.
69. Hyttel J, Fredricson O, Arnt J. Biochemical effects and drug levels in rats after long-term treatment with the specific 5-HT-uptake inhibitor, citalopram. *Psychopharmacology* 1984;83:20–27.
70. Dewar KM, Grondin L, Nénonéné EK, Ohayon M, Reader TA. [^{3}H]paroxetine binding and serotonin content of rat brain: absence of changes following antidepressant treatments. *Eur J Pharmacol* 1993;235:137–142.
71. Graham D, Tahraoui L, Langer SZ. Effect of chronic treatment with selective monoamine oxidase inhibitors and specific 5-hydroxytryptamine uptake inhibitors on [^{3}H]paroxetine binding to cerebral cortical membranes of the rat. *Neuropharmacology* 1988;26:1087–1092.
72. Kovachich GB, Aronson CE, Brunswick DJ. Effect of repeated administration of antidepressants on serotonin uptake sites in limbic and neocortical structures of rat brain determined by quantitative autoradiography. *Neuropsychopharmacology* 1992;7:317–324.
73. Dewar KM, Grondin L, Carli M, Lima L, Reader TA. [^{3}H]paroxetine binding and serotonin content of rat cortical areas, hippocampus, neostriatum, ventral mesencephalic tegmentum, and midbrain raphe nuclei region following p-chlorophenylalanine and p-chloroamphetamine treatment. *J Neurochem* 1992;58:250–257.
74. Kimelberg HK. Occurrence and functional significance of serotonin and catecholamine uptake by astrocytes. *Biochem Pharmacol* 1986;14:2273–2281.
75. Zigmond MJ, Acheson AL, Stachowiak MK, Stricker EM. Neurochemical compensation after nigrostriatal bundle injury in an animal model of preclinical parkinsonism. *Arch Neurol* 1984;41:856–861.